

# Vertebrate Epidermal Cells Are Broad-Specificity Phagocytes That Clear Sensory Axon Debris

Jeffrey P. Rasmussen,<sup>1</sup> Georgeann S. Sack,<sup>1</sup> Seanna M. Martin,<sup>1</sup> and Alvaro Sagasti<sup>1</sup>

Department of Molecular, Cell and Developmental Biology, University of California, Los Angeles, Los Angeles, California 90095

Cellular debris created by developmental processes or injury must be cleared by phagocytic cells to maintain and repair tissues. Cutaneous injuries damage not only epidermal cells but also the axonal endings of somatosensory (touch-sensing) neurons, which must be repaired to restore the sensory function of the skin. Phagocytosis of neuronal debris is usually performed by macrophages or other blood-derived professional phagocytes, but we have found that epidermal cells phagocytose somatosensory axon debris in zebrafish. Live imaging revealed that epidermal cells rapidly internalize debris into dynamic phosphatidylinositol 3-monophosphate-positive phagosomes that mature into phagolysosomes using a pathway similar to that of professional phagocytes. Epidermal cells phagocytosed not only somatosensory axon debris but also debris created by injury to other peripheral axons that were mislocalized to the skin, neighboring skin cells, and macrophages. Together, these results identify vertebrate epidermal cells as broad-specificity phagocytes that likely contribute to neural repair and wound healing.

**Key words:** axon; phagocytosis; skin; somatosensory; Wallerian degeneration; zebrafish

## Introduction

The skin protects animals from environmental insults by functioning as both a physical barrier and a sensory organ. The outermost layers of skin, the epidermis, are densely innervated by axonal endings of somatosensory neurons, which intermingle with epithelial cells (for review, see Dubin and Patapoutian, 2010). Somatosensory axon endings degenerate following cutaneous injuries, leading to sensory abnormalities (Inbal et al., 1987; Healy et al., 1996; Theriault et al., 1998; Rajan et al., 2003). Repair of sensory endings in the epidermis is impaired in patients with peripheral neuropathies, such as those associated with human immunodeficiency virus or diabetes (Polydefkis et al., 2004; Hahn et al., 2007).

Clearance of cellular debris is a key step in tissue and nerve repair. In most cases, blood-derived professional phagocytes, including neutrophils, macrophages, and microglia, phagocytose neuronal debris (for review, see Vargas and Barres, 2007). Specialized nonprofessional phagocytes, such as peripheral glia (Stoll et al., 1989; Lewis and Kucenas, 2014) and the retinal pigment epithelium (RPE; Young and Bok, 1969), can phagocytose neuronal debris in specific contexts. Understanding how cutaneous sensory endings are repaired requires identifying the cell types

that clear axon debris in the skin. Although professional phagocytes play a major role in healing skin wounds, in *Caenorhabditis elegans* and *Drosophila* epidermal cells contribute to phagocytosis of apoptotic neurons and degenerating neurites (Robertson and Thomson, 1982; Hall et al., 1997; Han et al., 2014). Vertebrate epidermal cells can internalize melanosomes (for review, see Van Den Bossche et al., 2006), beads (Wolff and Konrad, 1972), bacteria (Åsbakk, 2001), and perhaps even cellular debris (Odland and Ross, 1968; Mottaz and Zelickson, 1970). However, whether they significantly contribute to phagocytosis and the degradation of debris during neural and cellular repair is unknown.

Axon degeneration and clearance in the zebrafish skin is a rapid and stereotyped process (Martin et al., 2010). If cutaneous axon degeneration is delayed, persistent axon fragments repel regenerating axons (Martin et al., 2010), implying that an understanding of the debris clearance process may ultimately suggest approaches for improving cutaneous reinnervation. Here we use the zebrafish system to provide the first description of the fate of axon debris in the vertebrate skin.

## Materials and Methods

**Zebrafish.** Zebrafish (*Danio rerio*) were grown at 28.5°C on a 14 h/10 h light/dark cycle. Embryos were raised at 28.5°C in fish water (0.3 g/L Instant Ocean Salt, 0.1% methylene blue). The following zebrafish strains were used: AB (wild-type), *nacre* (*nac<sup>w2</sup>*) (Lister et al., 1999), *leo1<sup>la1186</sup>* (Nguyen et al., 2010), and *cloche* (*clo<sup>m39</sup>*) (Stainier et al., 1995). The following previously described transgenes were used: *Tg(isl1[ss]:Gal4-VP16,UAS:DsRed)<sup>z234</sup>* (O'Brien et al., 2009), *Tg(mpeg1:mCherry)<sup>g123</sup>* (Ellett et al., 2011), *Tg(lyz:EGFP)<sup>nz117</sup>* (Hall et al., 2007), *Tg(UAS:Lifact-GFP)<sup>mu271</sup>* (Helker et al., 2013), *Tg(krt5:EGFP)<sup>ncc100</sup>* (Hu et al., 2010), *Tg(Tru.p2rx3a:LEXA-VP16,4xLEXAop:mCherry)<sup>Ja207</sup>* (Palanca et al., 2013), *TgBAC(neurod:EGFP)<sup>m11</sup>* (Obholzer et al., 2008), *Tg(krt4:DsRed)<sup>Ja203</sup>* (O'Brien et al., 2012), and *Tg(h2afx:EGFP-rab5c)<sup>mw5</sup>*, *Tg(h2afx:EGFP-rab7)<sup>mw7</sup>*, and *Tg(UAS:mCherry-rab5c S34N)<sup>mw33</sup>* (Clark et

Received Aug. 26, 2014; revised Sept. 26, 2014; accepted Oct. 14, 2014.

Author contributions: J.P.R. and A.S. designed research; J.P.R., G.S.S., and S.M.M. performed research; J.P.R. and A.S. analyzed data; J.P.R. and A.S. wrote the paper.

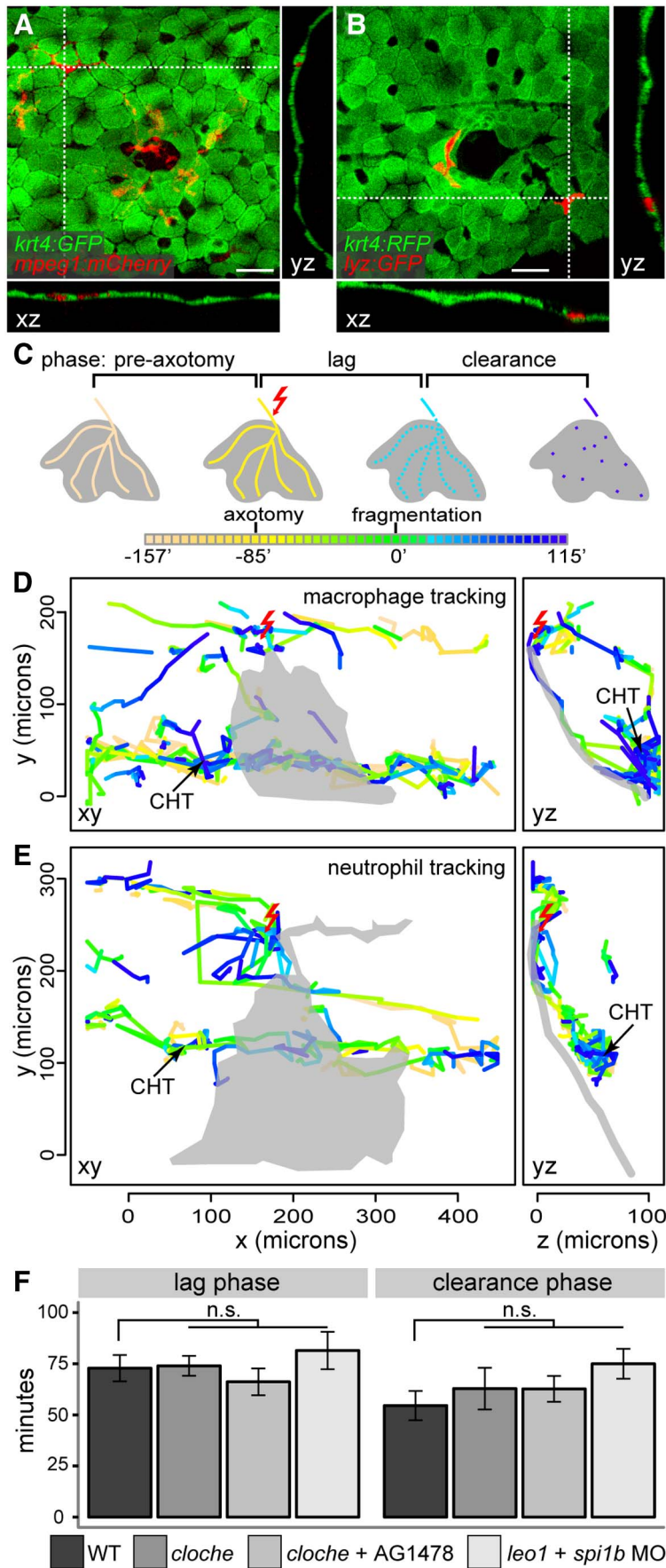
This work was supported by a grant from the Jane Coffin Childs Fund (to J.P.R.) and Grant R01AR064582 from the National Institutes of Health (to A.S.). We thank B. Link, H. Stenmark, M. Halpern, W. Herzog, M. Veldman, A. Nechiporuk, D. Raible, S. Schulte-Merker, K. Kawakami, and M. Suster for sharing reagents; the laboratories of L. Iruela-Arispe, J.-N. Chen, and S. Lin for access to equipment; members of the Sagasti laboratory for advice; and S. Basenfelder for fish care.

The authors declare no competing financial interests.

Correspondence should be addressed to either Jeffrey P. Rasmussen or Alvaro Sagasti, 621 Charles E. Young Drive South, Los Angeles, CA 90095. E-mail: rasmuss@ucla.edu or sagasti@mcdb.ucla.edu.

DOI:10.1523/JNEUROSCI.3613-14.2015

Copyright © 2015 the authors 0270-6474/15/350559-12\$15.00/0



al., 2011). Zebrafish of either sex were used for this study. All experiments using zebrafish were approved by the University of California, Los Angeles (UCLA) Chancellor's Animal Research Committee.

**Plasmid construction.** Plasmid cloning was performed using the Gateway-based Tol2Kit (Kwan et al., 2007). The following plasmids have been described previously: p5E-4xUASnr (Akitake et al., 2011), p5E-*krt4* (O'Brien et al., 2012), pME-*LEXA-VP16,4xLEXAop* (Palanca et al., 2013), pME-*EGFP*, p3E-*EGFP-polyA*, p3E-*polyA*, and pDestTol2pA2 (Kwan et al., 2007). The *neurod:mTangerine* plasmid was a gift from Alex Nechiporuk (Oregon Health & Science University, Portland, OR). The entry vectors p5E-*krt5*, p5E-*krt11c19e*, p5E-*isl1[ss]*, pME-*Gal4FF*, pME-*EGFP-2xFYVE*, pME-*lamp1*, and p3E-*tdTomato* were cloned by recombining PCR products into pDONR P4-P1R (p5E), pDONR 221 (pME), or pDONR P2R-P3 (p3E). The following oligonucleotides and templates were used in plasmid construction: p5E-*krt5* (5'-GGGGCAACTTGTATAGAAAAGTTGGCACAACCTAACGCACTCTGC-3', 5'-GGGGACTGCTTTTTTGTACAAAAGTTGGGTGAGGATCAGAAAAAGAGCA-3'; zebrafish genomic DNA; Hu et al., 2010); p5E-*krt11c19e* (5'-GGGGACAACCTTGTATAGAAAAGTTGCAACAACAATCCACCTCAAGAGT-3', 5'-GGGGGACTGCTTTTTGTGTACAAAAGTTGGATGGTGGTGGTGTCTTACTCT-3'; zebrafish genomic DNA; Lee et al., 2014); p5E-*isl1[ss]* (5'-GGGGACAACTTGTATAGAAAAGTTGCTCGAGCCTCGGCTCAGTT-3', 5'-GGGGACTGCTTTTGTGTACAAAAGTTGGAATCTGACACA GAATTGAATTG-3'; *isl1[ss]:Gal4-VP16, UAS:GFP* plasmid; Sagasti et al., 2005); pME-*Gal4FF* (5'-GGGGACAAGTTTGTACAAA AAAGCAGGCTGCCACCATGAAGCTAC TGCTTCTATC-3', 5'-GGGGACCACTTT

←

**Figure 1.** Leukocytes do not associate with degenerating peripheral arbors. **A, B**, Confocal images of the trunk of transgenic zebrafish larvae at 3 dpf showing the epidermis [*Tg(krt4:RFP)* or *Tg(krt4:EGFP)*] in green and macrophages [*Tg(mpeg1:mCherry)*] or neutrophils [*Tg(lyz:EGFP)*] in red. **C**, Experimental schematic showing axotomy and degeneration of a peripheral sensory axon in the skin. The innervated territory is gray. Throughout the article, 0 min represents the time of axon fragmentation. **D, E**, Representative tracings of leukocyte behavior before and after axotomy. Leukocyte tracks are colored according to the phase of axon degeneration, as indicated in **C**. A single somatosensory peripheral axon was axotomized in 2 dpf zebrafish transgenic for either *Tg(mpeg1:mCherry)* (**D**) or *Tg(lyz:EGFP)* (**E**). The red arrow points to the axotomy site. The caudal hematopoietic tissue (CHT) is indicated. **F**, Quantification of the lag and clearance phases following axotomy of single somatosensory peripheral axons at 54 hpf in the indicated genetic backgrounds. The durations of the lag and clearance phases were unaffected by the removal of leukocytes [*cloche* or *spi1b* morpholino (MO)] or peripheral glia (AG1478 or *leo1*). Data are represented as the mean  $\pm$  SEM. n.s., Not significant ( $p > 0.16$ ; one-way ANOVA with Dunnett's *post hoc* test).  $n = 7$ –12 for each condition. Scale bars, 50  $\mu$ m.

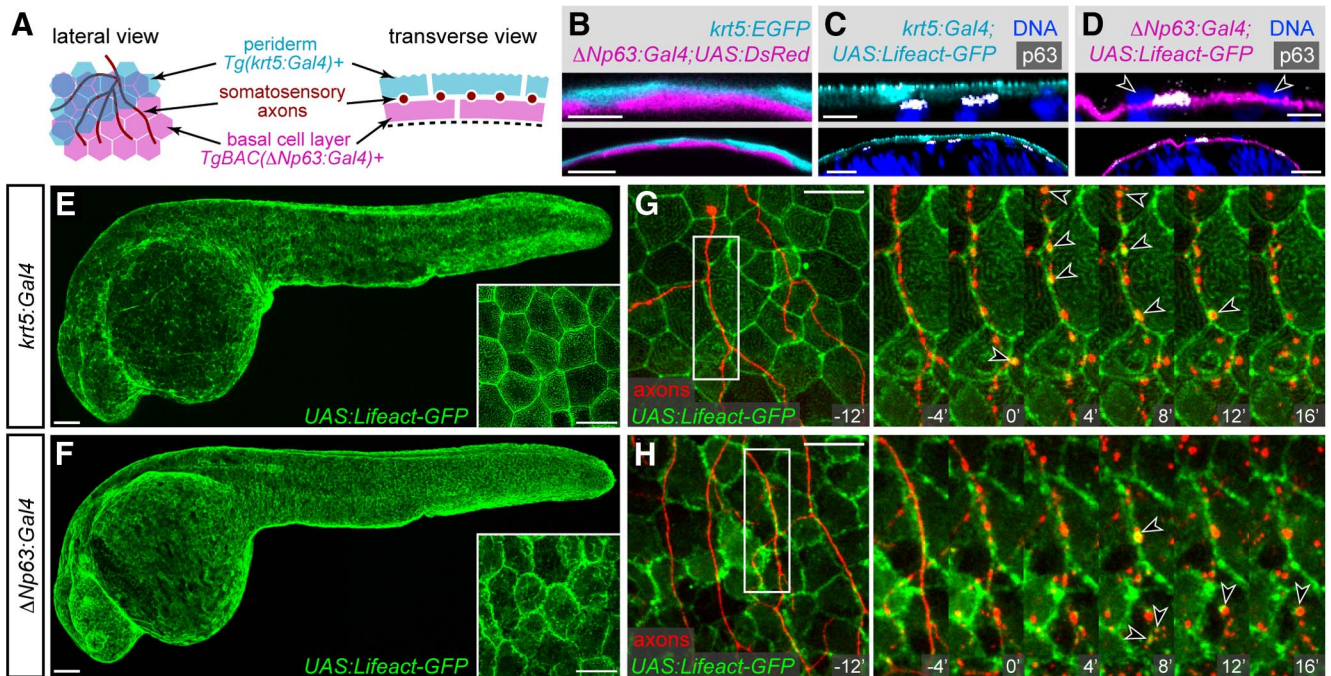


**Figure 2.** Epidermal actin dynamics during axon degeneration. **A**, Diagram showing larval epidermal anatomy in relation to somatosensory peripheral axons. Dashed line represents the basement membrane underlying the epidermis. **B–D**, Single optical sections showing transverse views of the periderm (cyan) and basal cells (magenta) in transgenic larvae. The top panels are higher-magnification views of the bottom panels. **C, D**, Reconstructed cross sections of animals fixed at 30 hpf and immunostained with anti-GFP and anti-p63 antibodies. p63 staining (white) shows the basal cell nuclei, and DAPI staining (blue) shows all nuclei. In **C**, note that the GFP-expressing periderm cells are superficial to the p63-positive basal cell layer. In **D**, the arrowheads indicate periderm nuclei superficial to the GFP- and p63-positive basal cell layer. **E, F**, Confocal images of transgenic larva fixed at 30 hpf and immunostained with an anti-GFP antibody. Insets show higher-magnification lateral views of the epidermis. **G, H**, Lateral confocal images from time-lapse imaging series showing F-actin dynamics in periderm (**G**) and basal cells (**H**) following transection of an axon (red) at 32 hpf. Arrowheads indicate transient enrichments of F-actin around axon debris. See also Movie 1. Scale bars: **B–D** (top panels), 10  $\mu$ m; **B–D** (bottom panels), 25  $\mu$ m; **E, F**, 100  $\mu$ m; **E, F**, Insets, 25  $\mu$ m; **G, H**, 25  $\mu$ m.

GTACAAGAAAGCTGGGTTTAGTTACCCGGGAGCATATCG-3'; pCS2+<sub>Gal4FF</sub>\_kanR; Busmann and Schulte-Merker, 2011); pME-EGFP-2xFYVE (5'-GGGACAAGTTTGTACAAAAAAGCAGGCTA-ACCGGTGCCACCAT-3', 5'-GGGACCACCTTTGTACAAGAAA GCTGGGTTT CAGTTATCTAGATCCGGTGGATCC-3'); pEGFP-2xFYVE; Gillooly et al., 2000); pME-lamp1 (5'-GGGACAAGTTTGTACAAAAAAGCAGGCTGGACCATGGCGCGAGCTGCAGGTGTT TGC-3', 5'-GGGACCACCTTTGTACAAGAAAGCTGGGTAGATGG TCTGGTACCCGGCGTGTG-3'; zebrafish cDNA; a gift from Matt Veldman, UCLA); and p3E-tdTomato (5'-GGGACAGCTTTCTT GTACAAAGTGGGCGCCACCATGGTGAGCAAGGGCGAGGAG-3', 5'-GGGACAACCTTTGTATAATAAAGTTGTCACCTCGAGT GACCCAGATCTTCCACCGCCCTGTACAGCTCGTCCATGCC TA-3'; ChEF-tdTomato plasmid; Lin et al., 2009).

**Transgene generation.** The  $\Delta$ Np63:Gal4FF bacterial artificial chromosome (BAC) was created by modifying BAC DKEY-263P13, which contains 117.9 kb upstream and 19.0 kb downstream of the  $\Delta$ Np63 $\alpha$  open reading frame (ENSDART0000065137). *iTol2-amp* was recombined into the backbone of DKEY-263P13, and the predicted  $\Delta$ Np63 start codon was replaced by a *Gal4FF*-*polyA*-*KanR* cassette using a previously described protocol (Suster et al., 2011). *Tg(krt4:EGFP)*<sup>la211</sup>, *Tg(krt5:Gal4FF)*<sup>la212</sup>, *TgBAC(ΔNp63:Gal4FF)*<sup>la213</sup>, *Tg(4xUAS:EGFP-2xFYVE)*<sup>la214</sup>, and *Tg(isl1[ss]:LEXA-VP16,LEXAop:tdTomato)*<sup>la215</sup> were created by the injection of *tol2* mRNA and either plasmid or BAC DNA into one-cell stage embryos and screening adults for germline transmission. At least two founders were identified for each transgene. Transgenic strains have been outcrossed for at least two generations.

**Immunohistochemistry and lysotracker staining.** Immunohistochemistry was performed essentially as described previously (Webb et al., 2007). Briefly, embryos were dechorionated and fixed in 4% paraformaldehyde in PBS overnight at 4°C. Embryos were washed 3 × 5 min in 0.1% Triton X-100 in PBS (PBST), blocked for 1 h in 2% heat-inactivated goat serum, 2 mg/ml BSA in PBS, then incubated for 2 h with the appropriate primary

antibody. Primary antibodies were used at the following dilutions: mouse anti-p63, 1:100 (sc-8431, Santa Cruz Biotechnology); and rabbit anti-GFP, 1:500 (TP401, Torrey Pines Biolabs). Embryos were washed 4 × 15 min in PBST then incubated for 2 h in secondary antibody. Alexa Fluor 568-conjugated goat anti-mouse and Alexa Fluor 488-conjugated goat anti-rabbit secondary antibodies (Life Technologies) were diluted 1:500 in blocking solution. Embryos were washed 4 × 15 min in PBST. To visualize nuclei, embryos were incubated for 5 min in 5 ng/ $\mu$ l DAPI in PBS, followed by 4 × 5 min washes in PBST.

For lysotracker staining, animals were immersed in 10  $\mu$ M LysoTracker Deep Red (Life Technologies) and 1% DMSO for 45 min, and then washed several times in Ringer's solution (116 mM NaCl, 2.9 mM KCl, 1.8 mM CaCl<sub>2</sub>, and 5 mM HEPES, pH 7.2).

**Confocal microscopy.** Unless stated otherwise, images are maximum-intensity projections and were acquired by time-lapse microscopy using a laser-scanning microscope. Most imaging was performed on an LSM 510 confocal microscope (Carl Zeiss) equipped with a heated stage (PeCon) set to 28°C and 20× air [0.5 numerical aperture (NA)], 40× oil (1.3 NA), and 63× water (0.9 NA) objectives.

**Ablations.** Animals were anesthetized in 0.02% tricaine and embedded in 1.2% low-melt agarose; and microscope chambers were filled with Ringer's solution and sealed with vacuum grease. Ablations were performed on an LSM 510 META microscope (Carl Zeiss) equipped with a multiphoton laser (Coherent) using either a 25× water (0.8 NA) or 40× oil (1.3 NA) objective. The ablated region was specified using a 60–100× digital zoom and damaged with one to three scans of 813 nm light at 12–20% power.

**Plasmid and morpholino injections.** The *spi1b* antisense morpholino (Rhodes et al., 2005) was purchased from GeneTools, LLC. One-cell stage embryos were injected with 1–2 nl of *spi1b* morpholino at a concentration of 0.5 mM. For plasmid injections, 3–5 nl of DNA were injected into one-cell stage embryos at a concentration of 10–20 ng/ $\mu$ l. Unless stated otherwise, somatosensory axons were visualized using *Tg(isl1[ss]:LEXA-*

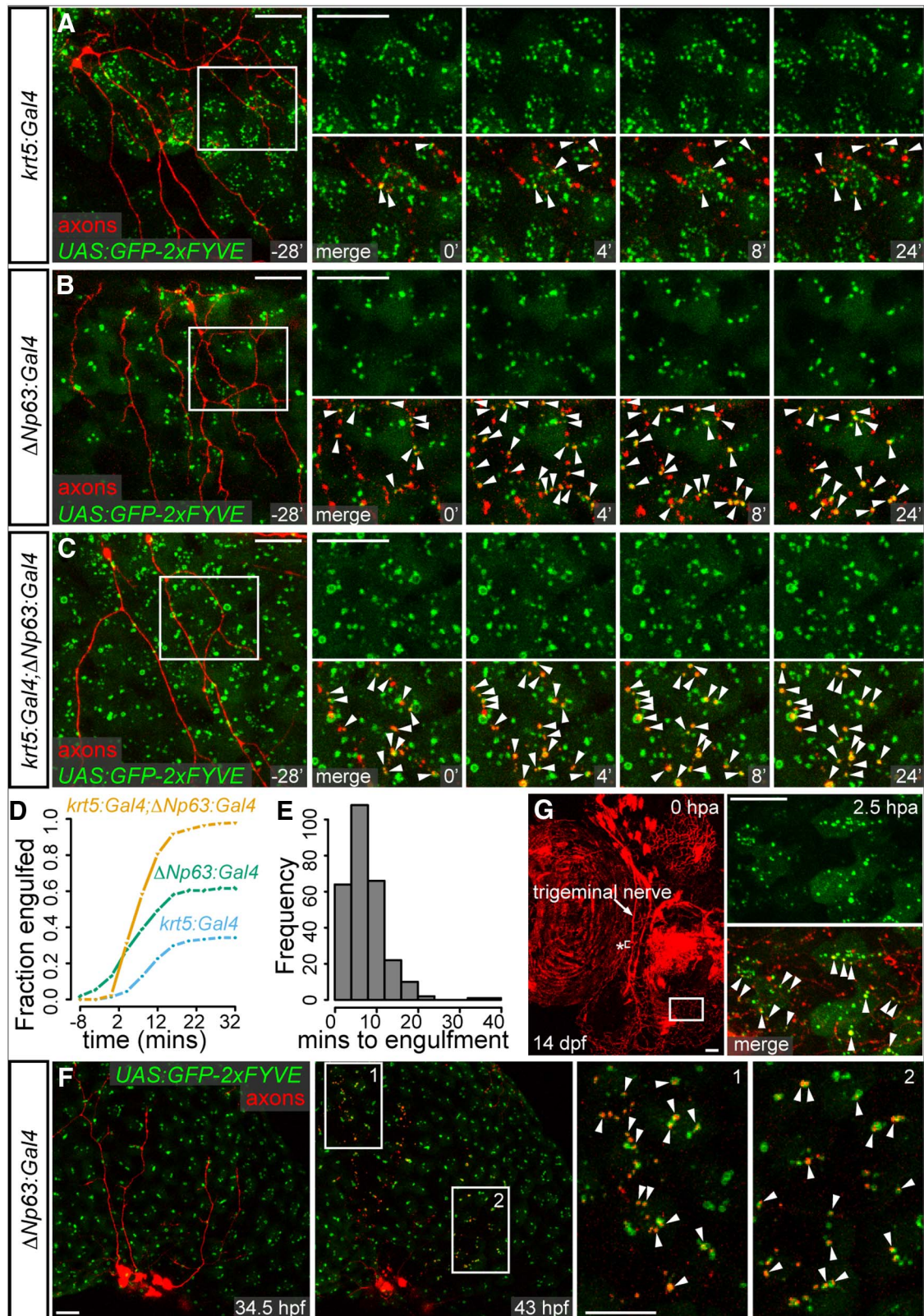


**Figure 3.** Both epidermal layers phagocytose axon debris. **A–C**, Confocal images of a phagosome reporter (green) expressed in periderm (**A**), basal cells (**B**), or both (**C**), following transection of an axon (red) at 32 hpf. In these and subsequent panels, arrowheads indicate phagosomes containing axon debris. See also Movie 2. **D**, The fraction of axon debris internalized, as assessed using the indicated Gal4 drivers and *Tg(UAS:GFP-2xFYVE)*. Data were pooled from at least two independent experiments and at least 164 fragments tracked per genotype. **E**, The time to internalization of axon debris by the epidermis in *Tg(krt5:Gal4); TgBAC(\Delta Np63:Gal4); Tg(UAS:GFP-2xFYVE)* transgenic animals. **F**, Phagocytosis of axon debris following spontaneous cell death. **G**, Axotomy of trigeminal axons in a *nacre; Tg(Tru.p2rx3a:LEXA-VP16,4xLEXAop:mCherry); TgBAC(\Delta Np63:Gal4); Tg(UAS:GFP-2xFYVE)* 14 dpf transgenic animal. Asterisk indicates the site of the axotomy. Right-hand panels are higher-magnification images of the boxed region. hpa, hours post axotomy. Scale bars, 25  $\mu$ m.

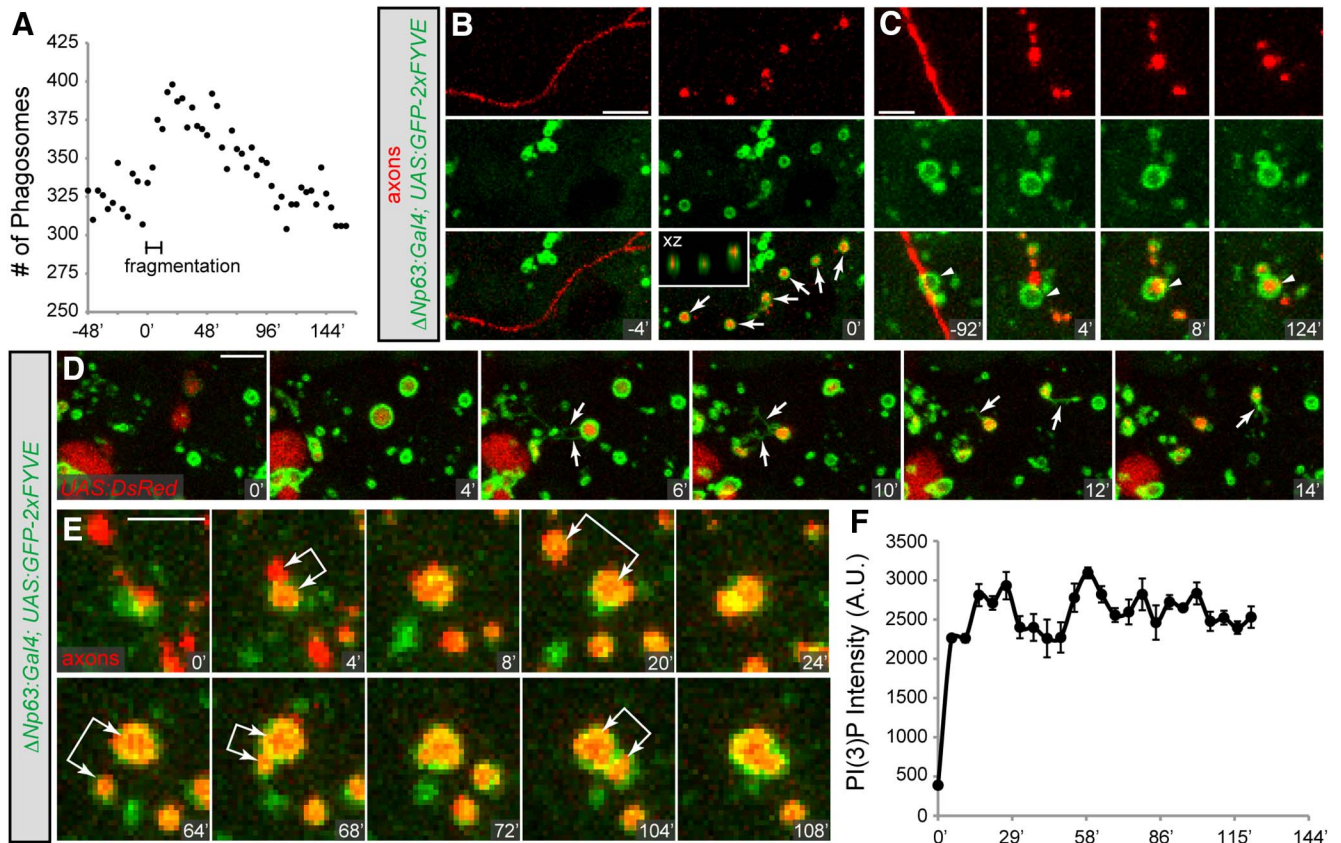


**Figure 4.** PI(3)P dynamics in the epidermis. Analysis of phagosomes in *TgBAC(ΔNp63:Gal4); Tg(UAS:GFP-2xFYVE)* transgenic larvae. **A**, Quantification of phagosome number in a 0.028 mm<sup>2</sup> region of the epidermis before and after axon fragmentation. **B**, Biogenesis of phagosomes (green) following axon (red) fragmentation. Arrows indicate newly formed phagosomes. Inset shows that phagosome membranes completely surround axon debris. **C**, An axon fragment (red) enters a pre-existing phagosome (green; arrowhead). **D**, Phagosomes (green) following phagocytosis of basal cell debris (red). Arrows indicate tubules extending from phagosomes following debris internalization. **E**, Fusion of phagosomes (green) containing somatosensory axon debris (red). Double-headed arrows indicate four sequential fusion events within a single cell. **F**, Quantification of PI(3)P intensity around phagocytosed axon debris ( $n = 3$  fragments). Note the two peaks of PI(3)P intensity at 26.5 and 58 min are separated by a gap period (~20 min) of decreased fluorescence. Data are represented as the mean  $\pm$  SEM. A.U., arbitrary units. Ablations were performed at 32 (**A**, **C**, **E**), 50 (**F**), 56 (**B**), or 74 (**D**) hpf. Scale bars, 5  $\mu$ m.

VP16, *LEXAop:tdTomato*) or by injection of an *isl1[ss]:LEXA-VP16, LEXAop:tdTomato* plasmid.

**Drug treatment.** For ErbB inhibitor experiments, embryos were bathed in fish water supplemented with 4  $\mu$ M AG1478 (Calbiochem) and 1% DMSO beginning at 8 h postfertilization (hpf). Animals treated with 1% DMSO were used as controls.

**Image analysis and statistics.** Images were analyzed using ImageJ (Schneider et al., 2012). Leukocyte tracking in Figure 1 was performed using the TrackMate plugin and plotted using R (<http://www.R-project.org>). The whole-embryo images in Figure 2, *E* and *F*, were made using the Pairwise Stitching plugin. To assess the amount and timing of axon debris engulfment in Figure 3, *D* and *E*, individual debris fragments were followed using the Manual Tracking plugin. Only debris that could be tracked for at least 12 min was analyzed. The Squash plugin was used to count phagosomes in Figure 4*A*. Quantifications in Figures 4*F*, 5*B*, and 6, *C* and *D*, were performed by tracing a region of interest (ROI) around individual axon fragments using the Freehand tool and measuring fluorescence intensity and area within the ROI. Unless otherwise stated, at least 10 debris fragments were analyzed per time point. Statistical tests were performed using the R software package.

## Results

### Leukocytes are not required for clearance of cutaneous debris

Laser axotomy of cutaneous axon endings in larval zebrafish causes the severed axon arbor to fragment through a process known as Wallerian degeneration (WD), creating axon debris in the epidermis (Martin et al., 2010; O'Brien et al., 2012). Since

most studies of axon debris clearance following WD have implicated blood-derived professional phagocytes in this process, we hypothesized that these cell types also clear axon debris in the skin. To determine whether blood-derived cells can penetrate into the epidermis, we imaged larvae double transgenic for an epidermal marker and a marker of either neutrophils or macrophages. Consistent with a previous study (Herbomel et al., 2001), both types of leukocytes were found in the epidermis of unmanipulated animals (Fig. 1*A, B*).

To characterize the behavior of neutrophils and macrophages following axon damage, we axotomized cutaneous endings, and imaged leukocyte behavior before and after WD (Fig. 1*C*). As expected, both cell types responded to injury by migrating to the site of laser damage (Fig. 1*D, E*). However, neither cell type interacted significantly with degenerating peripheral arbor (Fig. 1*D, E*). To test whether blood-derived cells were required for the clearance of cutaneous debris, we examined the rate of axon fragmentation and clearance in *cloche* mutants, which lack all blood cells (Stainier et al., 1995). Consistent with our imaging results, removal of blood cells did not alter the rate of fragmentation or debris clearance (Fig. 1*F*). Because peripheral glia can also phagocytose axon debris, we repeated these experiments impairing the development of both blood cells and peripheral glia, but again detected no significant difference in the rate of debris clearance compared with controls (Fig. 1*F*). These results indicate that

neither leukocytes nor peripheral glia are primary phagocytes for cutaneous axon debris.

### Actin dynamics in the epidermis during axon degeneration and debris clearance

The observation that neither blood-derived cells nor peripheral glia are required for cutaneous axon debris clearance led us to hypothesize that another cell type in the epidermis clears this debris. The larval zebrafish epidermis is a bilayered epithelium, consisting of an outer periderm and inner basal cell layer (Le Guellec et al., 2004), between which sensory axons arborize (Fig. 2*A,B*; O'Brien et al., 2012). We previously found that epidermal epithelial cells extend pseudopodia that contact degenerating axon debris (O'Brien et al., 2012). These pseudopodia are reminiscent of actin-rich phagocytic cups formed during phagocytosis of apoptotic corpses in *C. elegans* and opsonized beads by cultured macrophages (Swanson et al., 1999; Kinchen et al., 2005).

To visualize actin dynamics in both epithelial layers, we created Gal4 drivers specific to each and crossed them to the filamentous actin (F-actin) reporter *Tg(UAS:Lifeact-GFP)* (Fig. 2*C–F*; Helker et al., 2013). In both the periderm and basal cells, F-actin was transiently enriched around axon debris following fragmentation (Fig. 2*G,H*; Movie 1). Unlike the larval *Drosophila* epidermis, which accumulates actin around degenerating cutaneous dendrites before fragmentation (Han et al., 2014), we did not observe F-actin recruitment in either cell layer until after axon fragmentation (Fig. 2*G,H*; Movie 1), suggesting that in the zebrafish skin epidermal actin does not promote axon degeneration but may play a role in debris clearance.

### Both layers of the epidermis phagocytose axon debris

The above observations revealed that the epidermis forms phagocytic cup-like structures around axon debris, prompting us to hypothesize that the epidermis phagocytoses this debris. To test this idea, we created a transgenic reporter for phagosomes, *Tg(UAS:GFP-2xFYVE)*, based on the fusion of GFP to a tandem repeat of the FYVE domain of Hrs, which has previously been shown to bind phosphatidylinositol 3-monophosphate [PI(3)P; Gillooly et al., 2000], a phospholipid enriched on the surface of endosomes and phagosomes. Crossing the periderm-specific Gal4 driver to *Tg(UAS:GFP-2xFYVE)* revealed spherical structures reminiscent of endosomes/phagosomes (Fig. 3*A*). Following injury of cutaneous axon endings, periderm cells internalized fragmented axon debris into these PI(3)P-positive phagosomes (Fig. 3*A,D*). Crossing the basal cell driver to the PI(3)P reporter demonstrated that basal cells also internalized axon debris into phagosomes (Fig. 3*B,D*). Together, the two epithelial layers ac-

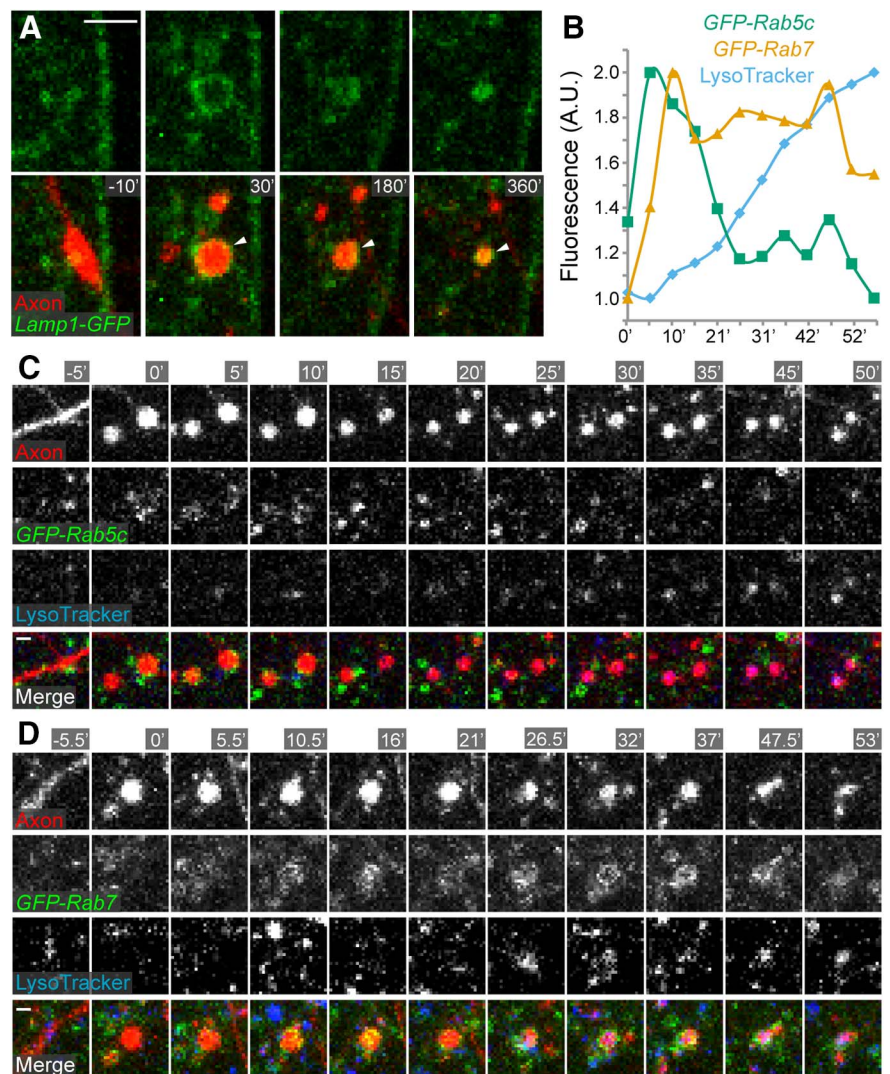


**Figure 5.** The endocytic pathway degrades debris in the epidermis. **A**, A periderm cell expressing *krtt1c19e:lamp1-GFP* (green) engulfs axon debris (red) in a *Tg(isl1[ss]:Gal4-VP16,UAS:DsRed)* transgenic animal. Arrowhead indicates a shrinking axon fragment that associates with Lamp1-GFP for several hours. **B**, Quantification of fluorescence intensity associated with axon debris over time. Data are represented as means. **C, D**, Confocal time-lapse images of axon debris phagocytosis in *Tg(h2afx:EGFP-rab5c)* (**C**) and *Tg(h2afx:EGFP-rab7)* (**D**) transgenic animals stained with lysotracker. Axons were transected at 32 (**A**) or 50 (**B, C, D**) hpf. Scale bars: **A**, 5  $\mu$ m; **C, D**, 1  $\mu$ m.

counted for phagocytosis of at least 98% of axon debris ( $n = 274/279$  fragments; Fig. 3*C,D*; Movie 2). Phagocytosis of axon debris by skin cells was rapid. The majority of debris was internalized into PI(3)P-positive phagosomes within 8 min of fragmentation (Fig. 3*E*). Axon debris created by spontaneous cell death was also internalized by the epidermis (Fig. 3*F*), indicating that this process is not specific to laser-induced injury.

A previous study found that cells with the stellate morphology characteristic of Langerhans cells, blood-derived professional phagocytes resident to vertebrate skin (Carrillo-Farga et al., 1990; Lugo-Villarino et al., 2010), populate the zebrafish epidermis by 12 d postfertilization (dpf; Wittamer et al., 2011). To determine whether epidermal cells still participate in clearance when these other phagocytic cells are present, we repeated these experiments at a later stage. Basal cells were still robustly phagocytic in 14 dpf animals (Fig. 3*G*). Together, these experiments identify epidermal cells as the primary phagocytes of cutaneous axon debris during development and following injury in zebrafish.

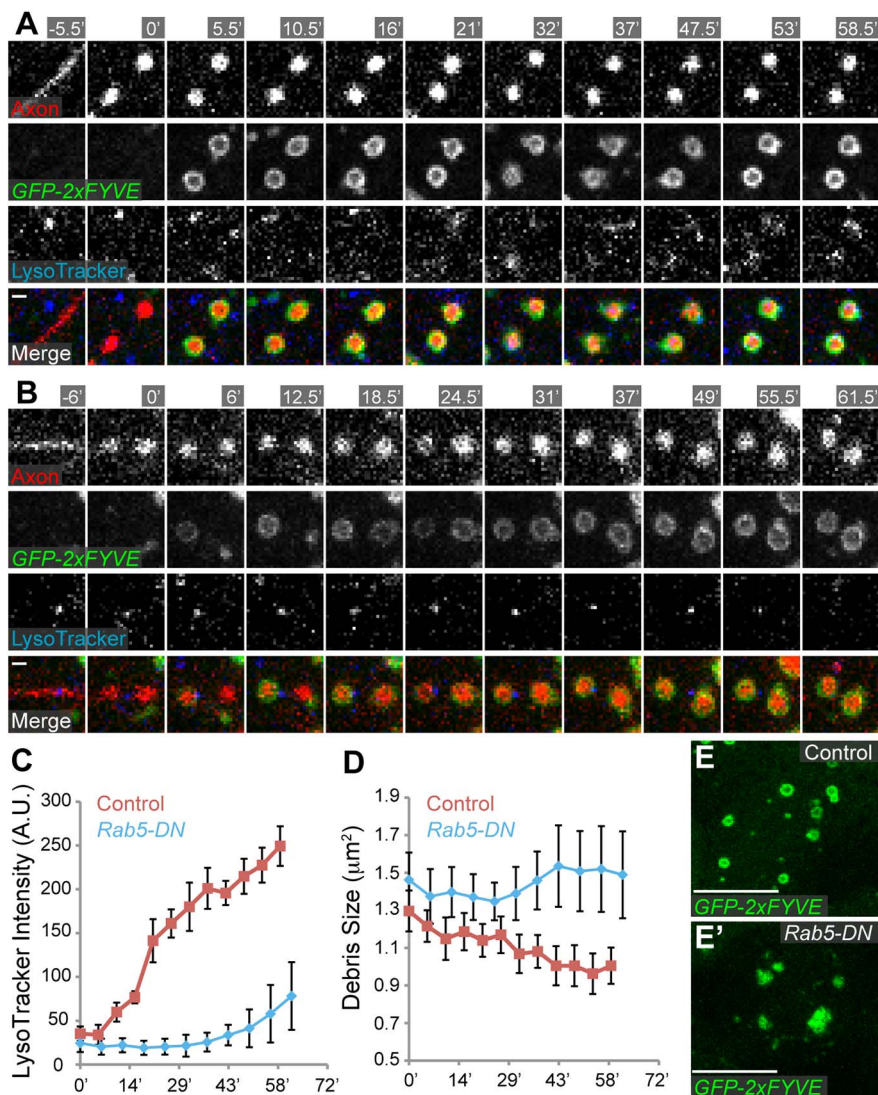


**Figure 6.** Rab5 activity is required for debris degradation by the epidermis. **A, B**, Confocal time-lapse images of *TgBAC(ΔNp63:Gal4); Tg(UAS:GFP-2xFYVE)* (**A**) and *TgBAC(ΔNp63:Gal4); Tg(UAS:GFP-2xFYVE); Tg(UAS:mCherry-rab5c S34N)* (**B**) transgenic animals stained with lysotracker. Axons were transected at 50 hpf. **C–E**, Analysis of phagocytosis in control and Rab5-DN animals. Transgenes are as in **A** (control) and **B** (Rab5-DN). **C, D**, Quantification of lysotracker intensity (**C**) and debris size (**D**) over time. Data are represented as the mean  $\pm$  SEM. **E, E'**, Confocal images showing phagosome aggregation in Rab5-DN-expressing cells at 2 dpf. Scale bars, **A, B**, 1  $\mu$ m; **E, E'**, 10  $\mu$ m.

### Phagosome dynamics in the epidermis

PI(3)P-positive phagosomes are highly dynamic during phagocytosis of apoptotic corpses in *C. elegans* (Yu et al., 2008; Lu et al., 2012) but have not been well characterized in other *in vivo* systems. Our ability to perform time-lapse imaging of skin cells in live zebrafish with high temporal and spatial resolution allowed us to characterize phagosome dynamics. Similar to phagocytosis in *C. elegans*, the formation of axon debris during WD promoted the biogenesis of new PI(3)P-positive compartments, which completely surrounded axon debris (Fig. 4*A, B*). However, unlike corpse phagocytosis, debris also entered pre-existing PI(3)P-positive compartments (Fig. 4*C*). Once formed, PI(3)P-positive phagosomes often fused together (Fig. 4*E*), a process that was observed in the *Drosophila* skin in *croquemort* mutants (Han et al., 2014). Sometimes phagosomes extended dynamic tubules (Fig. 4*D*), which are similar to those observed during *C. elegans* corpse engulfment (Yu et al., 2008). PI(3)P levels on the surface of axon debris-containing phagosomes appeared to oscillate

(Figs. 4*F, 6A*), which is reminiscent of the two waves of PI(3)P recruitment to phagosomes observed in *C. elegans* (Lu et al., 2012). Thus, zebrafish skin cells provide a facile model for monitoring the dynamics of phagocytosis in live animals.

### Trafficking of axon debris through the phagolysosomal pathway requires the small GTPase Rab5

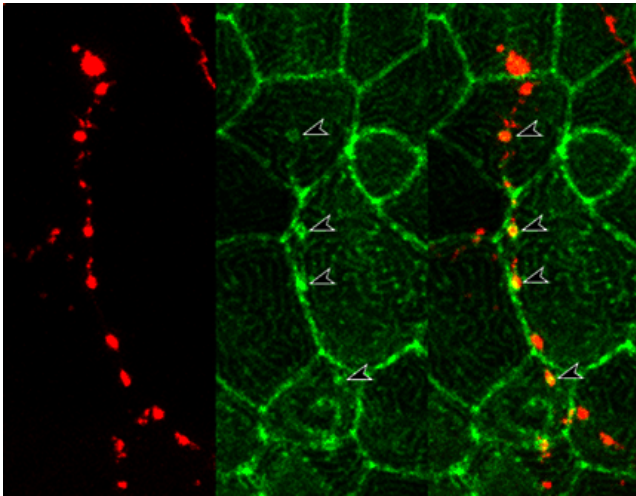
Basal skin cells in humans internalize melanosomes using a nonlytic vesicular pathway (for review, see Van Den Bossche et al., 2006). By contrast, phagosomes in *C. elegans* and mammalian macrophages mature through increasingly acidic compartments, ultimately resulting in the formation of a phagolysosome and lysis of the phagosome contents (for review, see Flannagan et al., 2012). To determine whether epidermal phagocytosis is mechanistically similar to either of these processes, we tested whether internalized axon debris associated with phagolysosomes by expressing Lamp1-GFP, a phagolysosome reporter, in epidermal cells. Lamp1-GFP surrounded axon debris as it became progressively smaller (Fig. 5*A*), indicating that skin cells degrade fragmented axons.

Phagosome maturation in invertebrate phagocytes and cultured macrophages requires sequential recruitment and activation of the small GTPases Rab5 and Rab7 (Kinchen et al., 2008; Han et al., 2014). Fluorescent fusion reporters of Rab5 and Rab7 (Clark et al., 2011) were rapidly and sequentially recruited to axon debris following fragmentation (Fig. 5*B–D*). Staining live animals with lysotracker, a marker of acidic organelles, revealed that phagosome acidification correlated with the loss of Rab5 association and a decrease in debris size (Fig. 5*B, C*). To test whether Rab5 activation is required for phagosome

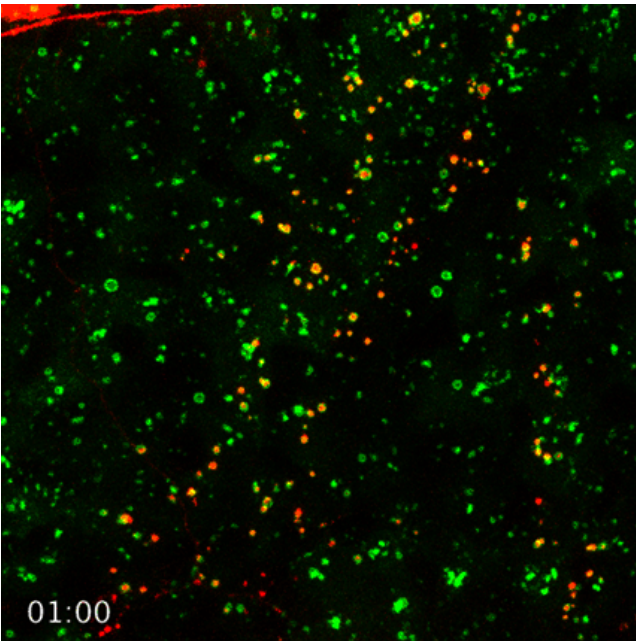
acidification, we expressed a dominant-negative version of Rab5 (Rab5-DN), engineered to have reduced GTP affinity (Clark et al., 2011), in basal cells and imaged axon debris. Rab5-DN-expressing basal cells internalized debris, but PI(3)P recruitment was inefficient (Fig. 6*A, B*). Moreover, phagosome acidification was delayed and debris size failed to decrease (Fig. 6*C, D*), although fluorescent debris eventually disappeared (data not shown). Rab5-DN expression also led to the clustering of PI(3)P-positive vesicles, consistent with a defect in phagosome fusion (Fig. 6*E*). Together, these data demonstrate that skin cells use mechanisms similar to professional phagocytes to degrade axon debris.

### Epidermal phagocyte specificity is determined by proximity

Phagocytic cells other than blood-derived professional phagocytes are sometimes termed “nonprofessional” phagocytes and are thought to be specialized to recognize specific types of debris (for review, see Rabinovitch, 1995). Do molecular signals specify



**Movie 1.** F-Actin dynamics in the epidermis during axon degeneration. F-actin dynamics in a *Tg(krt5:Gal4); Tg(UAS:Lifeact-GFP)* transgenic animal (green) following axotomy of a somatosensory peripheral axon (red) at 32 hpf. Arrowheads indicate enrichments of F-actin around axon debris. Frames were acquired every 4 min for 128 min.



**Movie 2.** Both epidermal layers phagocytose virtually all axon debris. Debris from a degenerating somatosensory peripheral axon (red) is engulfed into epidermal cell phagosomes (green) in a *Tg(krt5:Gal4); TgBAC(ΔNp63:Gal4); Tg(UAS:GFP-2xFYVE)* transgenic animal following axotomy at 32 hpf. Time is displayed as HH:MM (hours:minutes).

debris/phagocyte interactions, or is specificity simply determined by accessibility? To address this question, we devised experiments to test whether epidermal cells can phagocytose debris from axons they do not normally encounter, and, conversely, if mislocalized somatosensory axon debris can be phagocytosed by other types of cells. In control animals, the posterior lateral line nerve (PLLn) is associated with Schwann cells that position it below the epidermis (Fig. 7A; Raphael et al., 2010). Leukocytes phagocytose PLLn debris during injury-induced WD (Villegas et al., 2012). Consistent with this finding, basal skin cells did not phagocytose PLLn debris in control animals (Fig. 7B). Inhibition of the ErbB signaling pathway blocks peripheral glial development, causing the PLLn to remain in close association with the epidermis (Fig.

7C; Lyons et al., 2005; Raphael et al., 2010). Following ErbB inhibition and PLLn axotomy, basal cells phagocytosed debris from injured PLLn axons (Fig. 7D), suggesting that skin cells are not limited to phagocytosing debris only from somatosensory axons.

To determine whether somatosensory axon debris can be cleared by phagocytes other than skin cells we overexpressed a dominant-negative version of the PTPRFb receptor (PTPRFb-DN) specifically in somatosensory neurons (Wang et al., 2012). This manipulation impairs sensory axon guidance to the skin, causing some peripheral axons to innervate internal tissues (Wang et al., 2012). Degeneration of PTPRFb-DN-expressing peripheral axons, whether within the skin or below the skin, exhibited similar axon fragmentation and debris clearance kinetics (Fig. 7E,F). This result suggests that epidermal cells are not required for fragmentation of touch-sensing neurites, as has been proposed in *Drosophila* (Han et al., 2014), and that nonepidermal phagocytes, likely leukocytes, are capable of clearing somatosensory axon debris. Thus, specificity of phagocytes for axon debris, at least for skin cells and somatosensory axons, is determined by proximity rather than by dedicated molecular determinants.

### Epidermal cells phagocytose a broad range of debris

The ability of skin cells to phagocytose debris from at least two axon populations prompted us to investigate whether they could also phagocytose debris from other kinds of cells. First, we tested whether they could cannibalize debris of other epidermal cells by laser-ablating basal skin cells mosaically expressing DsRed in transgenic fish that expressed the PI(3)P reporter in all basal cells. Strikingly, much of the debris from these cells was internalized into phagosomes in neighboring basal cells (Fig. 8A). Similarly, debris from macrophages that were ablated in the skin was also phagocytosed by basal cells (Fig. 8B). Epidermal cells thus have broad phagocytic capabilities, suggesting that they may play roles not only in neural repair but also in wound healing.

### Discussion

Following developmental pruning or laser axotomy, cutaneous axon debris is rapidly removed from the zebrafish skin (Martin et al., 2010). The speed and reproducible timing of degeneration and clearance make zebrafish an excellent model for studying cutaneous repair. Surprisingly, we found that blood-derived phagocytes do not significantly interact with debris and are not required for debris removal, despite penetrating into the epidermis and responding to the site of injury. Instead, epithelial cells of the skin phagocytose axon debris. Combined with studies in *C. elegans* and *Drosophila* (Robertson and Thomson, 1982; Hall et al., 1997; Han et al., 2014), our results demonstrate that the ability of epidermal cells to phagocytose neuronal debris is conserved between vertebrates and invertebrates.

### Roles of vertebrate epidermal cells in neurite degeneration and clearance

The zebrafish epidermis shares many similarities with the mammalian epidermis and is significantly more complex than invertebrate skin. While invertebrate skin is typically a monolayer, zebrafish skin is initially bilayered and becomes increasingly stratified with the addition of suprabasal cells as the animal ages (Le Guellec et al., 2004). By developing transgenic tools specific to each layer of the larval epidermis, we found that both epithelial layers are phagocytic, with the basal cell layer eating the majority of the debris. Do suprabasal cells also eat axon debris in older animals? Recent studies found that stratification of zebrafish skin is remarkably similar to mammalian skin (Guzman et al., 2013;

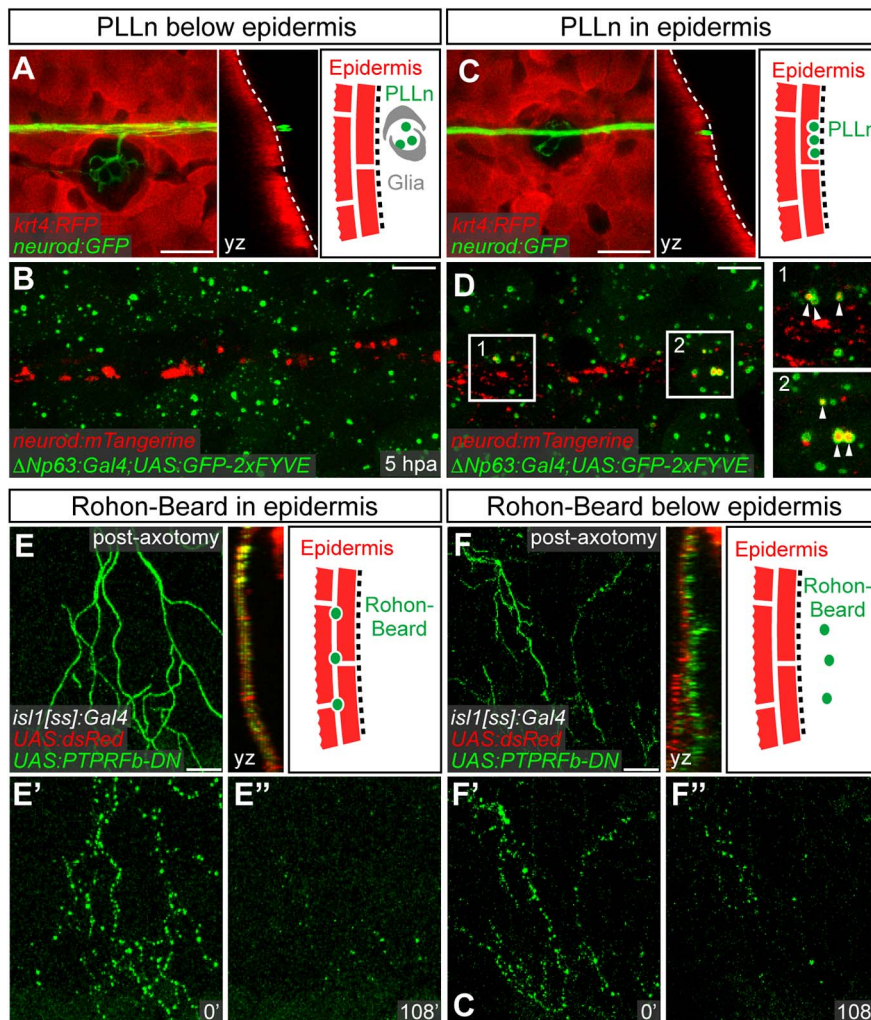


**Figure 7.** Epidermal cells phagocytose multiple types of neuronal debris, and neuronal debris is recognized by multiple phagocytes. **A, C**, Confocal images of the PLLn and epidermis at 3 dpf. Dashed line represents the basement membrane underlying the epidermis. **B, D**, Confocal images showing phagosomes (green) 5 hpa of the PLLn (red). Axotomy was performed at 74 hpf. **E, F**, Confocal images of single somatosensory axons expressing *PTPRFb-DN-GFP* following axotomy at 52 hpf. The duration of the lag phase (mean  $\pm$  SD) was  $126.2 \pm 23.4$  min for axons in epidermis ( $n = 9$ ) and  $135.4 \pm 16.2$  min for axons below ( $n = 10$ ;  $p = 0.342$ , unpaired two-tailed Student's *t* test). The duration of the clearance phase was  $130.0 \pm 44.9$  min for axons in epidermis ( $n = 9$ ) and  $150.8 \pm 61.2$  min for axons below ( $n = 10$ ;  $p = 0.408$ , unpaired two-tailed Student's *t* test). Scale bars: **A, C, E, F**, 25  $\mu$ m; **B, D**, 10  $\mu$ m.

Lee et al., 2014), but markers do not yet exist to specifically label suprabasal cells in zebrafish. Akin to other vertebrates, the zebrafish epidermis contains resident Langerhans cells (Lugo-Villarino et al., 2010). We found the epidermis is still robustly phagocytic after the differentiation of Langerhans cells, suggesting that the proliferation of Langerhans cells seen in experimental models of neuropathy and humans with small-fiber neuropathy (Lauria et al., 2005; Siau et al., 2006; Casanova-Molla et al., 2012) may be primarily related to tissue inflammation rather than debris clearance.

Studies in *Drosophila* have proposed that phagocytes not only clear cutaneous neurite debris, but also participate in neurite destruction (Williams and Truman, 2005; Han et al., 2014). A potential destruction mechanism involves the corpse engulfment receptor cell death abnormal-1 (CED-1)/Draper-dependent concentration of epidermal F-actin around neurites before fragmentation (Han et al., 2014). By imaging F-actin dynamics in the zebrafish skin, we found that F-actin did not associate with so-

matosensory axons before fragmentation. Moreover, axon fragmentation proceeded with normal kinetics after repositioning somatosensory axons below the skin. Thus, cutaneous neurite destruction may involve distinct mechanisms in vertebrates and invertebrates.

### Dynamics of phagocytosis in the epidermis

Phagocytosis of cellular debris requires specific particle recognition molecules, rearrangement of the phagocytic membrane, and pathways for internalization and trafficking. Phagocytes can use several types of receptors to recognize cellular debris (for review, see Flannagan et al., 2012). For example, the CED-1 family receptor Draper is used by *Drosophila* glial and epidermal cells to recognize neurite debris (Hoopfer et al., 2006; MacDonald et al., 2006; Han et al., 2014), whereas vertebrate RPE cells use the MerTK receptor to recognize photoreceptor debris (D'Cruz et al., 2000). We have yet to identify the receptor used by vertebrate epidermal cells to recognize debris, but since these cells can clear several different kinds of cellular debris, the receptor likely recognizes a universal signal of degenerating membranes.

A previous ultrastructural study (O'Brien et al., 2012) found that pseudopodia project from zebrafish epidermal cell membranes toward degenerating axon debris. Consistent with this study, live imaging revealed that epidermal cells concentrate F-actin in ring-like structures around axon debris shortly after fragmentation. These results indicate that epidermal cells rearrange their membranes into phagocytic cup-like structures around axon debris before internalization, similar to the phagocytosis of beads by cultured macrophages. Following particle recognition, the mechanisms used to internalize debris depend on particle size. For example, inhibition of PI3K (phosphatidylinositol 3-kinase) only affects phagocytosis of beads at least 3  $\mu$ m in diameter (Araki et al., 1996; Cox et al., 1999). Because WD generates cutaneous axon fragments of varying sizes ( $\sim 0.5$ –4  $\mu$ m in diameter; data not shown), it will be interesting to determine whether the mechanisms used to internalize axon debris are also size dependent.

Whereas professional phagocytes are highly motile, epidermal cells are not, making it possible to visualize the dynamics of progression through the phagolysosomal pathway *in vivo* with high resolution. The most extensively characterized *in vivo* system for phagocytosis is the clearance of apoptotic corpses during embryonic development in *C. elegans* (for review, see Li et al., 2013). We found that phagocytosis of axon debris shares many similarities with corpse clearance, including the generation of new phagosomal compartments upon debris internalization, oscillations of PI(3)P on the surface of phagosomes, and a requirement for Rab5 for the efficient recruitment of PI(3)P to phagosomes and debris

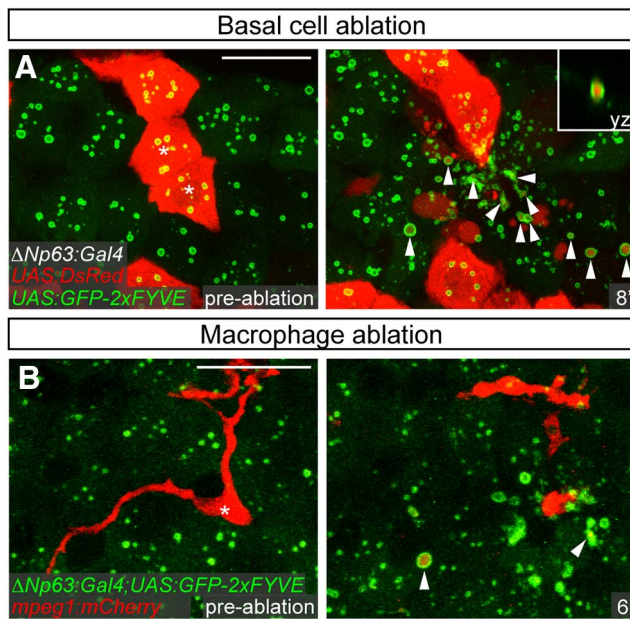


**Figure 8.** Epidermal cells are broad-specificity phagocytes. **A**, Confocal images before and after ablation of two basal cells mosaically expressing DsRed. Asterisks indicate ablated cells. Arrowheads indicate phagosomes containing basal cell debris. Inset shows that phagosome membranes completely surround basal cell debris. **B**, Confocal images before and after ablation of a single macrophage (red) in the epidermis. Asterisk indicates ablated cell. Arrowheads indicate phagosomes containing macrophage debris. Ablations were performed at 74 hpf. Scale bars, 25  $\mu$ m.

degradation. Phagocytes in the *C. elegans* embryo typically internalize only one apoptotic cell at a time; by contrast, epidermal cells in zebrafish can phagocytose multiple axon fragments per cell, and we observed the repeated fusion of phagosomal compartments containing axon debris. An upper limit on the amount of debris that individual skin cells can clear may exist, since a previous study found that creating large amounts of axon debris in the epidermis slowed debris degradation (Martin et al., 2010).

### Many cell types contribute to phagocytosis of neuronal debris

Although the phagocytic ability of Schwann cells and the RPE has long been recognized (Young and Bok, 1969; Stoll et al., 1989), recent work has shown that several other cell types, including astrocytes (Chung et al., 2013; Tasdemir-Yilmaz and Freeman, 2014), perineurial glia (Lewis and Kucenas, 2014), and the epidermis (this study; Han et al., 2014), play major roles in nervous system homeostasis. The ability of these nonprofessional phagocytes to process neuronal debris may have evolved as a specialization in response to the widespread death and remodeling of neurons during development and/or damage to neurons by injury later in life. Alternatively, phagocytosis may be an underappreciated, but near universal ability of many cell types. Since PLLn axon debris, which is normally cleared by leukocytes, was cleared by skin cells when genetically mispositioned to the skin, and, conversely, somatosensory axon debris was likely cleared by leukocytes when mispositioned below the skin, phagocytosis of specific types of neuronal debris is not limited to a single cell type. These observations are consistent with several paradoxical findings that removal of the primary phagocyte does not necessarily delay axon debris clearance (Perry et al., 1995; Villegas et al., 2012; Niemi et al., 2013).

The free endings of somatosensory axons are extremely large and complex, often orders of magnitude larger than other axonal

endings in the skin (Wu et al., 2012). Understanding the mechanisms involved in maintaining these somatosensory endings is important for the prevention and treatment of peripheral neuropathies. The ability to visualize and manipulate somatosensory debris clearance in a living, intact vertebrate may lead to improved regenerative treatments. Moreover, since the phagocytic nature of the skin is not limited to neuronal debris, it may have important implications for other forms of tissue repair.

### References

- Akitake CM, Macurak M, Halpern ME, Goll MG (2011) Transgenerational analysis of transcriptional silencing in zebrafish. *Dev Biol* 352:191–201. CrossRef Medline
- Araki N, Johnson MT, Swanson JA (1996) A role for phosphoinositide 3-kinase in the completion of macropinocytosis and phagocytosis by macrophages. *J Cell Biol* 135:1249–1260. CrossRef Medline
- Åsbakk K (2001) Elimination of foreign material by epidermal malpighian cells during wound healing in fish skin. *J Fish Biol* 58:953–966. CrossRef Medline
- Bussmann J, Schulte-Merker S (2011) Rapid BAC selection for tol2-mediated transgenesis in zebrafish. *Development* 138:4327–4332. CrossRef Medline
- Carrillo-Farga J, Castell A, Pérez A, Rondán A (1990) Langerhans-like cells in amphibian epidermis. *J Anat* 172:39–45. Medline
- Casanova-Molla J, Morales M, Planas-Rigol E, Bosch A, Calvo M, Grau-Junyent JM, Valls-Solé J (2012) Epidermal Langerhans cells in small fiber neuropathies. *Pain* 153:982–989. CrossRef Medline
- Chung WS, Clark LE, Wang GX, Stafford BK, Sher A, Chakraborty C, Joung J, Foo LC, Thompson A, Chen C, Smith SJ, Barres BA (2013) Astrocytes mediate synapse elimination through MEGF10 and MERTK pathways. *Nature* 504:394–400. CrossRef Medline
- Clark BS, Winter M, Cohen AR, Link BA (2011) Generation of Rab-based transgenic lines for in vivo studies of endosome biology in zebrafish. *Dev Dyn* 240:2452–2465. CrossRef Medline
- Cox D, Tseng CC, Bjekic G, Greenberg S (1999) A requirement for phosphatidylinositol 3-kinase in pseudopod extension. *J Biol Chem* 274:1240–1247. CrossRef Medline
- D’Cruz PM, Yasumura D, Weir J, Matthes MT, Abderrahim H, LaVail MM, Vollrath D (2000) Mutation of the receptor tyrosine kinase gene *Mertk* in the retinal dystrophic RCS rat. *Hum Mol Genet* 9:645–651. CrossRef Medline
- Dubin AE, Patapoutian A (2010) Nociceptors: the sensors of the pain pathway. *J Clin Invest* 120:3760–3772. CrossRef Medline
- Ellett F, Pase L, Hayman JW, Andrianopoulos A, Lieschke GJ (2011) *mpeg1* promoter transgenes direct macrophage-lineage expression in zebrafish. *Blood* 117:e49–56. CrossRef Medline
- Flannagan RS, Jaumouillé V, Grinstein S (2012) The cell biology of phagocytosis. *Annu Rev Pathol* 7:61–98. CrossRef Medline
- Gillooly DJ, Morrow IC, Lindsay M, Gould R, Bryant NJ, Gaullier JM, Parton RG, Stenmark H (2000) Localization of phosphatidylinositol 3-phosphate in yeast and mammalian cells. *EMBO J* 19:4577–4588. CrossRef Medline
- Guzman A, Ramos-Balderas JL, Carrillo-Rosas S, Maldonado E (2013) A stem cell proliferation burst forms new layers of P63 expressing suprabasal cells during zebrafish postembryonic epidermal development. *Biol Open* 2:1179–1186. CrossRef Medline
- Hahn K, Triolo A, Hauer P, McArthur JC, Polydefkis M (2007) Impaired reinnervation in HIV infection following experimental denervation. *Neurology* 68:1251–1256. CrossRef Medline
- Hall C, Flores MV, Storm T, Crosier K, Crosier P (2007) The zebrafish lysozyme C promoter drives myeloid-specific expression in transgenic fish. *BMC Dev Biol* 7:42. CrossRef Medline
- Hall DH, Gu G, García-Añoveros J, Gong L, Chalfie M, Driscoll M (1997) Neuropathology of degenerative cell death in *Caenorhabditis elegans*. *J Neurosci* 17:1033–1045. Medline
- Han C, Song Y, Xiao H, Wang D, Franc NC, Jan LY, Jan YN (2014) Epidermal cells are the primary phagocytes in the fragmentation and clearance of degenerating dendrites in *Drosophila*. *Neuron* 81:544–560. CrossRef Medline
- Healy C, LeQuesne PM, Lynn B (1996) Collateral sprouting of cutaneous nerves in man. *Brain* 119:2063–2072. CrossRef Medline
- Helker CS, Schuermann A, Karpanen T, Zeuschner D, Belting HG, Affolter

- M, Schulte-Merker S, Herzog W (2013) The zebrafish common cardinal veins develop by a novel mechanism: lumen ensheathment. *Development* 140:2776–2786. [CrossRef Medline](#)
- Herbomel P, Thisse B, Thisse C (2001) Zebrafish early macrophages colonize cephalic mesenchyme and developing brain, retina, and epidermis through a M-CSF receptor-dependent invasive process. *Dev Biol* 238:274–288. [CrossRef Medline](#)
- Hoopfer ED, McLaughlin T, Watts RJ, Schuldiner O, O’Leary DD, Luo L (2006) Wlds protection distinguishes axon degeneration following injury from naturally occurring developmental pruning. *Neuron* 50:883–895. [CrossRef Medline](#)
- Hu B, Zhang C, Baawo K, Qin R, Cole GJ, Lee JA, Chen X (2010) Zebrafish K5 promoter driven GFP expression as a transgenic system for oral research. *Oral Oncol* 46:31–37. [CrossRef Medline](#)
- Inbal R, Rouso M, Ashur H, Wall PD, Devor M (1987) Collateral sprouting in skin and sensory recovery after nerve injury in man. *Pain* 28:141–154. [CrossRef Medline](#)
- Kinchen JM, Cabello J, Klingele D, Wong K, Feichtinger R, Schnabel H, Schnabel R, Hengartner MO (2005) Two pathways converge at CED-10 to mediate actin rearrangement and corpse removal in *C. elegans*. *Nature* 434:93–99. [CrossRef Medline](#)
- Kinchen JM, Doukoumetzidis K, Almendinger J, Stergiou L, Tosello-Tramont A, Sifri CD, Hengartner MO, Ravichandran KS (2008) A pathway for phagosome maturation during engulfment of apoptotic cells. *Nat Cell Biol* 10:556–566. [CrossRef Medline](#)
- Kwan KM, Fujimoto E, Grabher C, Mangum BD, Hardy ME, Campbell DS, Parant JM, Yost HJ, Kanki JP, Chien CB (2007) The Tol2kit: a multisite gateway-based construction kit for Tol2 transposon transgenesis constructs. *Dev Dyn* 236:3088–3099. [CrossRef Medline](#)
- Lauria G, Lombardi R, Borgna M, Penza P, Bianchi R, Savino C, Canta A, Nicolini G, Marmiroli P, Cavaletti G (2005) Intraepidermal nerve fiber density in rat foot pad: neuropathologic-neurophysiologic correlation. *J Peripher Nerv Syst* 10:202–208. [CrossRef Medline](#)
- Lee RT, Asharani PV, Carney TJ (2014) Basal keratinocytes contribute to all strata of the adult zebrafish epidermis. *PLoS One* 9:e84858. [CrossRef Medline](#)
- Le Guellec D, Morvan-Dubois G, Sire JY (2004) Skin development in bony fish with particular emphasis on collagen deposition in the dermis of the zebrafish (*Danio rerio*). *Int J Dev Biol* 48:217–231. [CrossRef Medline](#)
- Lewis GM, Kucenas S (2014) Perineurial glia are essential for motor axon regrowth following nerve injury. *J Neurosci* 34:12762–12777. [CrossRef Medline](#)
- Li Z, Lu N, He X, Zhou Z (2013) Monitoring the clearance of apoptotic and necrotic cells in the nematode *Caenorhabditis elegans*. *Methods Mol Biol* 1004:183–202. [CrossRef Medline](#)
- Lin JY, Lin MZ, Steinbach P, Tsien RY (2009) Characterization of engineered channelrhodopsin variants with improved properties and kinetics. *Biophys J* 96:1803–1814. [CrossRef Medline](#)
- Lister JA, Robertson CP, Lepage T, Johnson SL, Raible DW (1999) nacre encodes a zebrafish microphthalmia-related protein that regulates neural-crest-derived pigment cell fate. *Development* 126:3757–3767. [Medline](#)
- Lu N, Shen Q, Mahoney TR, Neukomm LJ, Wang Y, Zhou Z (2012) Two PI 3-kinases and one PI 3-phosphatase together establish the cyclic waves of phagosomal PtdIns(3)P critical for the degradation of apoptotic cells. *PLoS Biol* 10:e1001245. [CrossRef Medline](#)
- Lugo-Villarino G, Balla KM, Stachura DL, Bañuelos K, Werneck MB, Traver D (2010) Identification of dendritic antigen-presenting cells in the zebrafish. *Proc Natl Acad Sci U S A* 107:15850–15855. [CrossRef Medline](#)
- Lyons DA, Pogoda HM, Voas MG, Woods IG, Diamond B, Nix R, Arana N, Jacobs J, Talbot WS (2005) *erbb3* and *erbb2* are essential for schwann cell migration and myelination in zebrafish. *Curr Biol* 15:513–524. [CrossRef Medline](#)
- MacDonald JM, Beach MG, Porpiglia E, Sheehan AE, Watts RJ, Freeman MR (2006) The *Drosophila* cell corpse engulfment receptor Draper mediates glial clearance of severed axons. *Neuron* 50:869–881. [CrossRef Medline](#)
- Martin SM, O’Brien GS, Portera-Cailliau C, Sagasti A (2010) Wallerian degeneration of zebrafish trigeminal axons in the skin is required for regeneration and developmental pruning. *Development* 137:3985–3994. [CrossRef Medline](#)
- Mottaz JH, Zelikson AS (1970) The phagocytic nature of the keratinocyte in human epidermis after tape stripping. *J Invest Dermatol* 54:272–278. [CrossRef Medline](#)
- Nguyen CT, Langenbacher A, Hsieh M, Chen JN (2010) The PAF1 complex component *Leo1* is essential for cardiac and neural crest development in zebrafish. *Dev Biol* 341:167–175. [CrossRef Medline](#)
- Niemi JP, DeFrancesco-Lisowitz A, Roldán-Hernández L, Lindborg JA, Mandell D, Zigmond RE (2013) A critical role for macrophages near axotomized neuronal cell bodies in stimulating nerve regeneration. *J Neurosci* 33:16236–16248. [CrossRef Medline](#)
- Obholzer N, Wolfson S, Trapani JG, Mo W, Nechiporuk A, Busch-Nentwich E, Seiler C, Sidi S, Söllner C, Duncan RN, Boehland A, Nicolson T (2008) Vesicular glutamate transporter 3 is required for synaptic transmission in zebrafish hair cells. *J Neurosci* 28:2110–2118. [CrossRef Medline](#)
- O’Brien GS, Martin SM, Söllner C, Wright GJ, Becker CG, Portera-Cailliau C, Sagasti A (2009) Developmentally regulated impediments to skin reinnervation by injured peripheral sensory axon terminals. *Curr Biol* 19:2086–2090. [CrossRef Medline](#)
- O’Brien GS, Rieger S, Wang F, Smolen GA, Gonzalez RE, Buchanan J, Sagasti A (2012) Coordinate development of skin cells and cutaneous sensory axons in zebrafish. *J Comp Neurol* 520:816–831. [CrossRef Medline](#)
- Odland G, Ross R (1968) Human wound repair. I. Epidermal regeneration. *J Cell Biol* 39:135–151. [CrossRef Medline](#)
- Palanca AM, Lee SL, Yee LE, Joe-Wong C, Trinh le A, Hiroyasu E, Husain M, Fraser SE, Pellegrini M, Sagasti A (2013) New transgenic reporters identify somatosensory neuron subtypes in larval zebrafish. *Dev Neurobiol* 73:152–167. [CrossRef Medline](#)
- Perry VH, Tsao JW, Fearn S, Brown MC (1995) Radiation-induced reductions in macrophage recruitment have only slight effects on myelin degeneration in sectioned peripheral nerves of mice. *Eur J Neurosci* 7:271–280. [CrossRef Medline](#)
- Polydefkis M, Hauer P, Sheth S, Sirdofsky M, Griffin JW, McArthur JC (2004) The time course of epidermal nerve fibre regeneration: studies in normal controls and in people with diabetes, with and without neuropathy. *Brain* 127:1606–1615. [CrossRef Medline](#)
- Rabinovitch M (1995) Professional and non-professional phagocytes: an introduction. *Trends Cell Biol* 5:85–87. [CrossRef Medline](#)
- Rajan B, Polydefkis M, Hauer P, Griffin JW, McArthur JC (2003) Epidermal reinnervation after intracutaneous axotomy in man. *J Comp Neurol* 457:24–36. [CrossRef Medline](#)
- Raphael AR, Perlin JR, Talbot WS (2010) Schwann cells reposition a peripheral nerve to isolate it from postembryonic remodeling of its targets. *Development* 137:3643–3649. [CrossRef Medline](#)
- Rhodes J, Hagen A, Hsu K, Deng M, Liu TX, Look AT, Kanki JP (2005) Interplay of *pu.1* and *gata1* determines myelo-erythroid progenitor cell fate in zebrafish. *Dev Cell* 8:97–108. [CrossRef Medline](#)
- Robertson AMG, Thomson JN (1982) Morphology of programmed cell death in the ventral nerve cord of *Caenorhabditis elegans* larvae. *J Embryol Exp Morphol* 67:89–100.
- Sagasti A, Guido MR, Raible DW, Schier AF (2005) Repulsive interactions shape the morphologies and functional arrangement of zebrafish peripheral sensory arbors. *Curr Biol* 15:804–814. [CrossRef Medline](#)
- Schneider CA, Rasband WS, Eliceiri KW (2012) NIH Image to ImageJ: 25 years of image analysis. *Nat Methods* 9:671–675. [CrossRef Medline](#)
- Siau C, Xiao W, Bennett GJ (2006) Paclitaxel- and vincristine-evoked painful peripheral neuropathies: loss of epidermal innervation and activation of Langerhans cells. *Exp Neurol* 201:507–514. [CrossRef Medline](#)
- Stainier DY, Weinstein BM, Detrich HW 3rd, Zon LI, Fishman MC (1995) *Cloche*, an early acting zebrafish gene, is required by both the endothelial and hematopoietic lineages. *Development* 121:3141–3150. [Medline](#)
- Stoll G, Griffin JW, Li CY, Trapp BD (1989) Wallerian degeneration in the peripheral nervous system: participation of both Schwann cells and macrophages in myelin degradation. *J Neurocytol* 18:671–683. [CrossRef Medline](#)
- Suster ML, Abe G, Schouw A, Kawakami K (2011) Transposon-mediated BAC transgenesis in zebrafish. *Nat Protoc* 6:1998–2021. [CrossRef Medline](#)
- Swanson JA, Johnson MT, Beningo K, Post P, Mooseker M, Araki N (1999) A contractile activity that closes phagosomes in macrophages. *J Cell Sci* 112:307–316. [Medline](#)
- Tasdemir-Yilmaz OE, Freeman MR (2014) Astrocytes engage unique molecular programs to engulf pruned neuronal debris from distinct subsets of neurons. *Genes Dev* 28:20–33. [CrossRef Medline](#)

- Theriault M, Dort J, Sutherland G, Zochodne DW (1998) A prospective quantitative study of sensory deficits after whole sural nerve biopsies in diabetic and nondiabetic patients. Surgical approach and the role of collateral sprouting. *Neurology* 50:480–484. [CrossRef Medline](#)
- Van Den Bossche K, Naeyaert JM, Lambert J (2006) The quest for the mechanism of melanin transfer. *Traffic* 7:769–778. [CrossRef Medline](#)
- Vargas ME, Barres BA (2007) Why is Wallerian degeneration in the CNS so slow? *Annu Rev Neurosci* 30:153–179. [CrossRef Medline](#)
- Villegas R, Martin SM, O'Donnell KC, Carrillo SA, Sagasti A, Allende ML (2012) Dynamics of degeneration and regeneration in developing zebrafish peripheral axons reveals a requirement for extrinsic cell types. *Neural Dev* 7:19. [CrossRef Medline](#)
- Wang F, Wolfson SN, Gharib A, Sagasti A (2012) LAR receptor tyrosine phosphatases and HSPGs guide peripheral sensory axons to the skin. *Curr Biol* 22:373–382. [CrossRef Medline](#)
- Webb AE, Sanderford J, Frank D, Talbot WS, Driever W, Kimelman D (2007) Laminin alpha5 is essential for the formation of the zebrafish fins. *Dev Biol* 311:369–382. [CrossRef Medline](#)
- Williams DW, Truman JW (2005) Cellular mechanisms of dendrite pruning in *Drosophila*: insights from in vivo time-lapse of remodeling dendritic arborizing sensory neurons. *Development* 132:3631–3642. [CrossRef Medline](#)
- Wittamer V, Bertrand JY, Gutschow PW, Traver D (2011) Characterization of the mononuclear phagocyte system in zebrafish. *Blood* 117:7126–7135. [CrossRef Medline](#)
- Wolff K, Konrad K (1972) Phagocytosis of latex beads by epidermal keratinocytes in vivo. *J Ultrastruct Res* 39:262–280. [CrossRef Medline](#)
- Wu H, Williams J, Nathans J (2012) Morphologic diversity of cutaneous sensory afferents revealed by genetically directed sparse labeling. *Elife* 1:e00181. [CrossRef Medline](#)
- Young RW, Bok D (1969) Participation of the retinal pigment epithelium in the rod outer segment renewal process. *J Cell Biol* 42:392–403. [CrossRef Medline](#)
- Yu X, Lu N, Zhou Z (2008) Phagocytic receptor CED-1 initiates a signaling pathway for degrading engulfed apoptotic cells. *PLoS Biol* 6:e61. [CrossRef Medline](#)